

Lawrence Berkeley National Laboratory

LBL Publications

Title

Proton and Neutron Excitations in Superdeformed $\{sup 150\}Tb$

Permalink

<https://escholarship.org/uc/item/8cq3365z>

Journal

Physical Review C, 52(1)

Authors

Fallon, P.
Beausang, C.W.
Asztalos, S.
et al.

Publication Date

1995-05-01



Lawrence Berkeley Laboratory

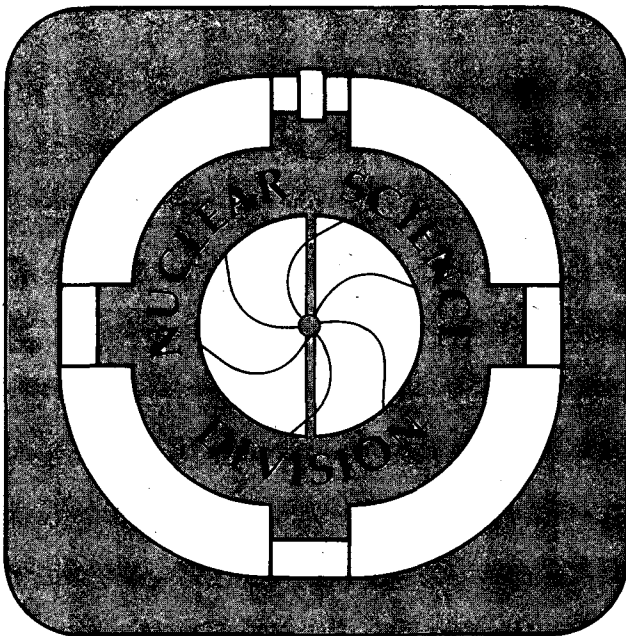
UNIVERSITY OF CALIFORNIA

Submitted to Physical Review C

Proton and Neutron Excitations in Superdeformed ^{150}Tb

P. Fallon, C.W. Beausang, S. Asztalos, D. Nisius, R.V.F. Janssens,
M. Bergstrom, M. Carpenter, B. Cederwall, S. Clarke, B. Crowell,
M.A. Deleplanque, R.M. Diamond, R.G. Henry, T.L. Khoo, T. Lauritsen,
I.Y. Lee, A.O. Macchiavelli, F.S. Stephens, and P.J. Twin

May 1995



REFERENCE COPY
Does Not
Circulate

Bldg. 50 Library.

LBL-37378

Copy 1

DISCLAIMER

This document was prepared as an account of work sponsored by the United States Government. While this document is believed to contain correct information, neither the United States Government nor any agency thereof, nor the Regents of the University of California, nor any of their employees, makes any warranty, express or implied, or assumes any legal responsibility for the accuracy, completeness, or usefulness of any information, apparatus, product, or process disclosed, or represents that its use would not infringe privately owned rights. Reference herein to any specific commercial product, process, or service by its trade name, trademark, manufacturer, or otherwise, does not necessarily constitute or imply its endorsement, recommendation, or favoring by the United States Government or any agency thereof, or the Regents of the University of California. The views and opinions of authors expressed herein do not necessarily state or reflect those of the United States Government or any agency thereof or the Regents of the University of California.

Proton and Neutron Excitations in Superdeformed ^{150}Tb

P. Fallon¹, C.W. Beausang², S. Asztalos¹, D. Nisius³,
R.V.F. Janssens³, M. Bergstrom², M. Carpenter³, B. Cederwall¹,
S. Clarke², B. Crowell³, M.A. Deleplanque¹, R.M. Diamond¹,
R.G. Henry³, T.L. Khoo³, T. Lauritsen³, I.Y. Lee¹, A.O. Macchiavelli¹,
F.S. Stephens¹, and P.J. Twin²

¹ *Nuclear Science Division, Lawrence Berkeley Laboratory
University of California, Berkeley, CA 94720, U.S.A.*

² *Oliver Lodge Laboratory, University of Liverpool, L69 3BX, United Kingdom.*

³ *Argonne National Laboratory, Argonne IL 60439, U.S.A.*

May 1995

This work was supported by the Director, Office of Energy Research Division
of Nuclear Physics of the Office of High Energy and Nuclear Physics of the
U.S. Department of Energy under Contract DE-AC03-76SF00098

Proton and Neutron Excitations in Superdeformed ^{150}Tb

P.Fallon¹, C.W.Beausang², S.Asztalos¹, D.Nisius³, R.V.F.Janssens³, M.Bergstrom²,
M.Carpenter³, B.Cederwall,¹ S.Clarke², B.Crowell³, M.A.Deleplanque¹, R.M.Diamond¹,
R.G.Henry³, T.L.Khoo³, T.Lauritsen³, I.Y.Lee¹, A.O.Macchiavelli¹, F.S.Stephens¹,
P.J.Twin².

¹ *Nuclear Science Division, Lawrence Berkeley Laboratory, Berkeley CA 94720, U.S.A.*

² *Oliver Lodge Laboratory, University of Liverpool, L69 3BX, United Kingdom.*

³ *Argonne National Laboratory, Argonne IL 60439, USA.*

Abstract

Two new superdeformed (SD) bands have been observed in ^{150}Tb using the reaction $^{31}\text{P} + ^{124}\text{Sn}$ and the GAMMASPHERE detector array. These new bands are interpreted as being excited SD configurations involving a proton and a neutron particle-hole excitation, respectively. The configurations are discussed in terms of the occupancy of high- N intruder orbitals. These data are used to provide information on: (i) the contribution to the dynamic moments of inertia due to the occupation of specific orbitals, (ii) the deformation driving effects of the particle-hole states, and (iii) the consequences of these effects on pairing and band-crossings.

21.10.Re, 23.20.Lv, 27.70 +q

I. INTRODUCTION

The spectroscopy of superdeformed (SD) nuclei ($\beta_2 \approx 0.6$) in the A=150 region began with the observation of a SD band in ^{152}Dy [1]. There are now over 40 SD bands reported in this region and in most cases their properties can be understood in terms of single-particle states in the absence of pair correlations. Exceptions to this are ^{150}Gd band 1 [2], ^{149}Gd band 2 [3,4], ^{144}Gd band 1 [5] and ^{150}Gd band 5 [6]¹ where the observation at low frequency of either (i) a rapid rise in the dynamic moment of inertia ($\mathfrak{S}^{(2)}$), or (ii) a backbend in the gamma-ray SD band transition energies, has been interpreted as a paired quasineutron or quasiproton band-crossing. In addition, more recent data on excited SD bands in ^{152}Dy [7] have been reported which the authors claim provide evidence for octupole (shape vibration) correlations.

In order to gain a better understanding of the role of correlations in A=150 SD bands (e.g., due to pair correlations or shape vibrations), one must first gain a better understanding of the role of specific single-particle states in determining the SD band properties. In particular the role of the high- N intruder orbitals has received a great deal of attention. At near spherical deformations ($\beta_2 \approx 0$) intruder orbitals are those which, due to the spin-orbit interaction, are lowered in energy from the $N + 1$ oscillator shell to the N^{th} shell. At superdeformations ($\beta_2 \approx 0.6$) levels originating from the $N+2$ oscillator shell appear close to the Fermi surface. The influence of these high- N intruder orbitals was first discussed by Bengtsson and co-workers [8] and later by Nazarewicz et al. [9]. It was found, for A=150 SD bands, that the $\mathfrak{S}^{(2)}$ moments of inertia are sensitive to the occupation of specific intruder orbitals. By comparing the calculated and experimental $\mathfrak{S}^{(2)}$ values it has been possible to assign intruder configurations to the SD bands and hence classify these nuclei by the number of intruder orbitals occupied.

¹The labelling of SD bands as band 1, band 2 etc. refers to the labelling adopted in the referenced works.

It is also important to obtain information on the non-intruder orbitals close to the Fermi surface. This becomes especially evident when one wishes to discuss the phenomenon of ‘identical’² SD bands [10–12]. For example, in the $A=150$ region, the occupation of the $\pi[301]1/2$, $\nu[411]1/2$ or the $\nu[514]9/2$ orbital has been linked with the observation of identical bands. An understanding of the single-particle properties of these and similar orbitals is therefore necessary.

In this paper we report data from an experiment to study the excited SD structures in the $N=85$, $Z=65$ nucleus ^{150}Tb . Two new SD bands are observed, which we interpret as excited SD bands in ^{150}Tb based on proton (band 2) and neutron (band 3) excitations relative to band 1 (the yrast SD band [13]). These data are used to provide information on (i) the contribution to the $\mathfrak{S}^{(2)}$ moments of inertia from the alignment of specific orbitals, (ii) the deformation driving effects of the particle-hole states, and (iii) the consequences of these effects on pairing and band-crossings, within the framework of cranked Woods-Saxon calculations.

II. EXPERIMENT

High-spin states in ^{150}Tb were produced at the Lawrence Berkeley Laboratory 88-inch cyclotron using the reaction $^{31}\text{P} + ^{124}\text{Sn}$ at a beam energy of 167 MeV. The target consisted of two isotopically enriched $600 \mu\text{g}/\text{cm}^2$ self-supporting foils. The subsequent gamma-ray decays were studied using the GAMMASPHERE detector array [14] which consisted at this time of 28 high resolution, $\sim 80\%$ efficient, escape-suppressed Ge detectors. The event trigger condition required at least 3 (Ge fold ≥ 3) escape-suppressed Ge detector signals to register in coincidence. The total number of events with Ge fold ≥ 3 was 1×10^9 which yielded

²In general, identical bands are those which have either integer or half-integer alignments relative to each other. The alignment is the difference in the total angular momenta at a given rotational frequency.

approximately 3×10^9 expanded triple events. Data analysis was carried out using both 3-dimensional $E_{\gamma_1}-E_{\gamma_2}-E_{\gamma_3}$ correlation cubes and single-gated 2-dimensional $E_{\gamma_1}-E_{\gamma_2}$ correlation matrices.

III. RESULTS AND DISCUSSION

In total, three SD bands have been observed in this data set, one of which (band 1) has been reported previously [13] and assigned as the yrast SD band in ^{150}Tb . In this experiment two new bands were assigned to ^{150}Tb through observed coincidences with low-lying normal deformed yrast ^{150}Tb transitions. The transition multipolarities in band 1 were shown [13] to be consistent with an E2 character. However, in this work we were not able to determine the multipolarity of transitions in bands 2 and 3 and the rotational nature of these bands, as well as their SD character, was inferred from the regular transition energy spacings and the intensity profiles. The transition energies and relative inband intensities are listed in table 1 for all three SD bands. Band 1 was found to carry $\sim 1\%$ of the total ^{150}Tb decay flux. The two new SD bands (bands 2 and 3) have intensities which are approximately 25% and 10% relative to that of band 1 respectively, and therefore we make the assumption that these bands are built on excited SD configurations. In the following sections we will concentrate on the properties and interpretations of the two new SD bands, and use the fact that the dynamic moments of inertia ($\mathfrak{S}^{(2)}$) are sensitive to the occupation of specific high- N intruder orbitals [8,9] in order to identify the most likely configurations for the two new SD bands in ^{150}Tb .

A. Band 1

The latest results for band 1 are presented for completeness and the spectrum is shown in Fig. 1. This band has been extended over the previous work [13] by two transitions. Fig. 2 shows the proton and neutron single-particle orbitals as a function of rotational frequency ($\hbar\omega$) for a fixed deformation $\beta_2 = 0.59$, $\beta_4 = 0.09$, appropriate for ^{150}Tb band 1 and taken

from ref. [9]. The calculations are based on a Woods-Saxon potential with the ‘universal’ parameters given in [15]. Band 1 in ^{150}Tb has been assigned [9,13] a $\pi 6^3\nu 7^1$ high- N intruder configuration (ie. three $N=6$ proton and one $N=7$ neutron intruder orbitals occupied).

It is clear from Fig. 2 that excited SD configurations (relative to band 1) may involve changes in either proton or neutron orbitals and more specifically changes in the occupation of the high- N intruder orbitals.

B. Band 2

The spectrum of band 2 is shown in Fig. 3 and its $\mathfrak{S}^{(2)}$ moment of inertia is plotted as a function of the rotational frequency in Fig. 4. Also included in Fig. 4 are the $\mathfrak{S}^{(2)}$ values for ^{151}Dy band 1 [16,17] (which is the $Z+1$ isotone of ^{150}Tb) and ^{150}Tb band 1 (dashed-line). Clearly, ^{150}Tb band 2 has a very different $\mathfrak{S}^{(2)}$ curve compared with ^{150}Tb band 1. Therefore, we do not associate band 2 with the same intruder configuration as ^{150}Tb band 1. We note, however, that the $\mathfrak{S}^{(2)}$ values in ^{150}Tb band 2 and ^{151}Dy band 1 exhibit a similar upward slope as a function of increasing $\hbar\omega$, and that their magnitudes differ by a roughly constant amount. Fig. 5 illustrates the contribution to the $\mathfrak{S}^{(2)}$ moment of inertia from the four lowest $N=6$ proton intruder orbitals (adapted from [8]). The favored signature of the $[651]3/2$ ($\alpha = +\frac{1}{2}$) proton intruder orbital (labelled $\pi 6_3$ in Fig. 5) generates a small and slightly decreasing contribution to the $\mathfrak{S}^{(2)}$ moment of inertia within the frequency range $\hbar\omega = 0.4 - 0.8$ MeV. Thus, it is proposed that the ^{150}Tb band 2 configuration can be described in terms of a hole in this orbital ($\pi 6_3$) relative to the ^{151}Dy band 1 core configuration (ie. $(^{151}\text{Dy})_{yrast} \otimes \pi([651]_{\frac{3}{2}})^{-1}$). This corresponds to a particle-hole excitation from the favored signature of the $[651]3/2$ ($\alpha = +\frac{1}{2}$) proton intruder orbital into the unfavored signature $[651]3/2$ ($\alpha = -\frac{1}{2}$), i.e., $\pi 6_3 \rightarrow \pi 6_4$. One may then describe ^{150}Tb band 2 as the unfavored signature partner to ^{150}Tb band 1. The reduced intensity of band 2 relative to band 1 is consistent with the large signature splitting for the $\pi[651]3/2$ orbital as shown in Fig. 2.

Recently [18], a similar proton excitation ($\pi 6_3 \rightarrow \pi 6_4$) has been proposed as an explanation for band 3 in ^{151}Tb . In this case, ^{151}Tb band 3 has a $\mathfrak{S}^{(2)}$ moment of inertia which exhibits a similar slope but with a reduced magnitude relative to that of ^{152}Dy band 1.

Other likely candidates for a simple particle-hole excitation involving proton orbitals would most likely require a hole in the $[301]1/2$ level. In analogy to the pair of identical bands in ^{152}Dy and $^{151}\text{Tb}^*$ [10], one may expect that an excited SD configuration in ^{150}Tb which involved the $[301]1/2$ orbital would result in a SD band with near identical transition energies relative to those observed in ^{151}Dy band 1. However, no SD band with these properties has been identified in this data set. This suggests that in ^{150}Tb , as compared with ^{151}Tb , the $[301]1/2$ orbital lies lower in energy relative to the $[651]3/2$ intruder level. Hence the $\pi 6_3 \rightarrow \pi 6_4$ excitation is more favorable.

C. Band 3

The spectrum of ^{150}Tb band 3 is shown in Fig. 6 and its $\mathfrak{S}^{(2)}$ moment of inertia, together with that for ^{151}Tb band 1, is shown in the upper part of Fig. 7 as a function of rotational frequency. In the lower part of Fig. 7 the $\mathfrak{S}^{(2)}$ curves for ^{149}Gd band 2 [4] and ^{150}Gd band 1 [2] are presented. For either the Gd or Tb isotope pair, the excited SD band in the $N=85$ nucleus exhibits a $\mathfrak{S}^{(2)}$ curve which falls below that of the yrast SD band in the $N=86$ isotope at the higher rotational frequencies. At low frequencies the excited SD bands (^{150}Tb band 3 and ^{149}Gd band 2) exhibit a $\mathfrak{S}^{(2)}$ which exceeds that seen in the $N+1$ yrast SD sequence (^{151}Tb band 1 and ^{150}Gd band 1). It is proposed that both ^{150}Tb and ^{149}Gd are associated with the same neutron particle-hole excitation and that this is most likely an excitation from a non-intruder $N=6$ orbital (either $[642]5/2$ or $[651]1/2$) to a $N=7$ high- N intruder ($[770]1/2$).

Since the interpretation for ^{150}Tb band 3 is closely related to that of ^{149}Gd band 2, it is instructive to discuss the Gd bands first. In ^{150}Gd band 1 – which has a $\pi 6^2\nu 7^2$ intruder configuration – the increase in $\mathfrak{S}^{(2)}$ at $\hbar\omega \approx 0.4$ (Fig. 7 lower) is associated [2] with a

$N=7$ quasineutron band-crossing. The ^{149}Gd SD band 2 configuration is assumed [3] to be based on a neutron particle-hole excitation from the $[642]5/2$ (or $[651]1/2$) orbital into the $N=7$ intruder orbital ($[(770)1/2 \alpha=+1/2]$). Therefore this band also has a $\pi 6^2\nu 7^2$ intruder configuration and the backbend in ^{149}Gd band 2 at $\hbar\omega \approx 0.45$ (Fig. 7 lower) is associated [3,4] with the same $N=7$ quasineutron band-crossing as observed in ^{150}Gd band 1. The differences in the $\mathfrak{S}^{(2)}$ curves at low frequency for ^{149}Gd band 2 and ^{150}Gd band 1 imply different interaction strengths for the $N=7$ band-crossing. This is most likely due to small differences in the SD band deformations. Total Routhian Surface calculations [9] predict a smaller deformation for ^{149}Gd band 2 ($\beta_2=0.575$) compared with ^{150}Gd band 1 ($\beta_2=0.585$) due to the deformation driving effects of the $[642]5/2$ (or $[651]1/2$) neutron orbital. It is suggested that the smaller deformation for ^{149}Gd band 2 compared with ^{150}Gd band 1 results in a smaller $N=86$ SD shell gap which leads to an increase in the neutron level density and hence increased pairing. In addition, the neutron Fermi level in ^{149}Gd lies closer to the $N=7$ intruder orbitals and the net result is a decrease in the interaction strength for the $N=7$ crossing.

In order to investigate the effect of small changes in deformation on the $N=7$ crossing we have performed cranked shell model calculations for the case of $N=86$ neutrons at 3 deformations ($\beta_2 = 0.60, 0.58$ and 0.56). The calculations shown in Fig. 8 are based on a cranked Woods-Saxon potential at a fixed deformation and with a constant BCS-pair field calculated at $\hbar\omega=0$ MeV. One clearly observes a large reduction in the interaction strength for the $N=7$ quasineutron crossing as the deformation is reduced from $\beta_2 = 0.6 \rightarrow \beta_2 = 0.56$.

From the comparison given in Fig. 7 and the discussion above it is suggested that ^{150}Tb band 3 can also be associated with the excitation of a neutron from either the $[642]5/2$ or $[651]1/2$ orbital into the $N=7$ intruder orbital. Therefore ^{150}Tb band 3 would have a $\pi 6^3\nu 7^2$ intruder configuration (identical to that of ^{151}Tb band 1) coupled to a hole in either the $[642]5/2$ or $[651]1/2$ neutron orbital. It is proposed that the sharp rise in the ^{150}Tb band 3 $\mathfrak{S}^{(2)}$ values – at $\hbar\omega \approx 0.45$ MeV – is due to a paired band-crossing involving the $N=7$ quasineutrons. In this scenario, the deformation driving effects of the neutron hole lead to

a smaller deformation for ^{150}Tb band 3 relative to ^{151}Tb band 1 resulting in an increase in the neutron pairing at low frequencies.

In general, the observation – at low frequency – of large increases in the dynamic moments of inertia, and/or backbends, is given as evidence for the presence of pair correlations in $A=150$ SD bands. The precise nature of these pair correlations, whether dynamic (vibrational) or static, remains unclear.

IV. SUMMARY

In summary, two new SD bands have been observed in ^{150}Tb . These have been interpreted as being based on excited SD configurations involving a proton and a neutron particle-hole excitation, respectively. Band 2 exhibits a slightly rising $\mathfrak{S}^{(2)}$ moment of inertia, as a function of increasing rotational frequency, with a slope similar to that observed in ^{151}Dy band 1. The proposed configuration for ^{150}Tb band 2 is a hole in the ^{151}Dy band 1 core configuration (ie. $(^{151}\text{Dy})_{yrast} \otimes \pi([651]_{\frac{3}{2}})^{-1}$), and corresponds to a $\pi 6_3 \rightarrow \pi 6_4$ excitation. Band 3 is associated with a neutron hole in the ^{151}Tb band 1 configuration, and is assumed to have a $\pi 6^3 \nu 7^2$ intruder configuration. The hole, in the $[642]5/2$ or $[651]1/2$ neutron orbital, is calculated to slightly reduce the deformation for ^{150}Tb band 3 (relative to ^{151}Tb band 1) which implies a smaller $N=86$ SD shell gap and an increase in the neutron pairing. The sharp rise in the $\mathfrak{S}^{(2)}$ moment of inertia at low frequency is thus interpreted as a $N=7$ quasineutron paired band-crossing.

V. ACKNOWLEDGEMENTS

The authors thank the operators and staff of the 88 cyclotron. Discussions with R.M.Clark are gratefully acknowledged. One of us (SC) acknowledges receipt of an SERC postgraduate fellowship during the course of this work. This work is supported in part by the Department of Energy, Nuclear Physics Division, under contract no. DE-AC03-76SF00098 and W-31-109-ENG-38.

REFERENCES

- [1] P.J.Twin *et al.*, Phys. Rev. Lett. **57**, 811 (1986).
- [2] P.Fallon *et al.*, Phys. Lett. **218B**, 137 (1989) and Phys. Lett. **257B**, 269(1991).
- [3] B.Haas *et al.*, Phys. Rev. **C42**, R1817 (1990).
- [4] S.Flibotte *et al.*, Phys. Rev. Lett. **71**, 688 (1993).
- [5] S.Lunardi *et al.*, Phys. Rev. Lett. **72**, 1427(1994).
- [6] P.Fallon *et al.*, Phys. Rev. Lett. **73**, 782 (1994).
- [7] P.J.Dagnal *et al.*, Phys. Lett. **335b**, 313 (1994).
- [8] T.Bengtsson, S.Åberg and I.Ragnarsson, Phys. Lett. **208B**, 39 (1989).
- [9] W.Nazarewicz, R.Wyss and A.Johnson, Nucl. Phys. **A503**, 285 (1989).
- [10] T.Byrski *et al.*, Phys. Rev. Lett. **64**, 1650 (1990).
- [11] W.Nazarewicz, P.J.Twin, P.Fallon and J.D.Garrett, Phys. Rev. Lett. **64**, 1654 (1990).
- [12] F.S.Stephens *et al.*, Phys. Rev. Lett. **64**, 2623 (1990);
Phys. Rev. Lett. **65**, 301 (1990).
- [13] M.A.Deleplanque *et al.*, Phys. Rev. Lett. **60**, 1626 (1989).
- [14] I.Y.Lee Nucl. Phys. **A520**, 641c (1990).
- [15] S.Cwiok, J.Dudek, W.Nazarewicz, J.Skalski and T.Werner, Computer Phys. Comm. **24**
379 (1987).
- [16] G.-E.Rathke, *et al.*, Phys. Lett. **B209**, 177 (1988).
- [17] D.Nisius, *et al.*, Phys. Lett., in press
- [18] B.Kharraja, *et al.*, Phys. Lett. **B341**, 268 (1995).

Table 1. Table of transition energies (keV) and inband relative intensities for the three SD bands in ^{150}Tb . For each band the intensities are normalized to the maximum intensity carried by that band.

^{150}Tb SD band 1		^{150}Tb SD band 2		^{150}Tb SD band 3	
E_γ	Intensity	E_γ	Intensity	E_γ	Intensity
596.8 (0.2)	0.26 (0.05)	662.5 (0.2)	0.64 (0.06)	877.0 (0.4)	0.68 (0.06)
647.4 (0.1)	0.57 (0.03)	716.1 (0.2)	0.88 (0.05)	888.3 (0.3)	0.78 (0.06)
697.7 (0.1)	1.02 (0.02)	769.7 (0.3)	1.10 (0.06)	929.4 (0.3)	1.08 (0.07)
748.2 (0.1)	1.04 (0.02)	823.5 (0.3)	1.15 (0.05)	977.0 (0.3)	0.88 (0.10)
799.2 (0.1)	1.02 (0.02)	877.3 (0.3)	0.93 (0.05)	1026.7 (0.5)	1.01 (0.10)
850.5 (0.1)	0.89 (0.03)	930.5 (0.2)	0.82 (0.05)	1077.0 (0.4)	1.08 (0.09)
902.1 (0.1)	1.01 (0.02)	983.7 (0.2)	0.97 (0.05)	1126.2 (0.3)	0.91 (0.08)
954.1 (0.1)	0.99 (0.02)	1037.9 (0.2)	0.91 (0.05)	1177.9 (0.5)	0.82 (0.08)
1006.9 (0.1)	0.98 (0.02)	1090.8 (0.3)	0.95 (0.05)	1229.7 (0.6)	1.03 (0.10)
1059.6 (0.1)	0.96 (0.02)	1143.1 (0.3)	0.64 (0.04)	1282.4 (0.6)	0.80 (0.10)
1112.4 (0.1)	0.90 (0.02)	1196.1 (0.3)	0.70 (0.05)	1333.3 (0.7)	0.65 (0.06)
1165.5 (0.1)	0.88 (0.02)	1247.6 (0.4)	0.47 (0.04)	1387.1 (0.9)	0.32 (0.05)
1218.8 (0.1)	0.90 (0.02)	1299.7 (0.4)	0.58 (0.04)	1440.5 (1.0)	0.20 (0.08)
1272.3 (0.1)	0.67 (0.02)	1351.4 (0.6)	0.52 (0.04)	[1494.0 (1.2)]	0.10 (0.05)
1326.4 (0.2)	0.48 (0.02)	1403.3 (0.8)	0.31 (0.03)		
1380.3 (0.2)	0.38 (0.02)	1453.0 (1.1)	0.17 (0.05)		
1434.9 (0.2)	0.24 (0.02)				
1489.4 (0.3)	0.17 (0.03)				
1544.1 (0.7)	0.10 (0.02)				
1599.6 (1.0)	0.05 (0.03)				

FIGURES

FIG. 1. Spectrum generated by a sum of E_γ - E_γ coincidence gates on transitions in ^{150}Tb SD band 1. A ‘★’ denotes known normal deformed transitions in ^{150}Tb .

FIG. 2. Neutron and proton single-particle energies as a function of rotational frequency ($\hbar\omega$) for a fixed deformation $\beta_2 = 0.59$, $\beta_4 = 0.09$. The routhians are labelled by, $\pi = +$, $\alpha = +1/2$ (solid lines); $\pi = +$, $\alpha = -1/2$ (dotted lines); $\pi = -$, $\alpha = +1/2$ (dot-dashed lines); $\pi = -$, $\alpha = -1/2$ (dashed lines).

FIG. 3. Spectrum generated by a sum of E_γ - E_γ coincidence gates on transitions in ^{150}Tb SD band 2. A ‘★’ denotes known normal deformed transitions in ^{150}Tb .

FIG. 4. Dynamic moments of inertia, as a function of rotational frequency, for ^{150}Tb band 2 (filled circles), ^{151}Dy band 1 (open squares) and ^{150}Tb band 1 (dashed line).

FIG. 5. Single-particle contributions to the dynamic moment of inertia ($\mathfrak{I}^{(2)}$) from the four lowest $N=6$ proton intruder orbitals (adapted from ref. [8]). The labels 1 and 2 (3 and 4) refer to the two signatures of the $[600]1/2$ ($[651]3/2$) orbital.

FIG. 6. Spectrum generated by a sum of E_γ - E_γ coincidence gates on transitions in ^{150}Tb SD band 3. A ‘★’ denotes known normal deformed transitions in ^{150}Tb .

FIG. 7. Dynamic moments of inertia as a function of rotational frequency for (Upper) ^{150}Tb band 3 (filled circles) and ^{151}Tb band 1 (open squares), and (Lower) ^{149}Gd band 2 (filled circles) and ^{150}Gd band 1 (open squares).

FIG. 8. Quasineutron energies as function of rotational frequency for neutron number $N=86$ at deformations of $\beta_2=0.60, 0.58, 0.56$ ($\beta_4=0.11, 0.10, 0.09$), illustrating the reduction in the interaction strength for the $N=7$ intruder paired band crossing, as the deformation is reduced.

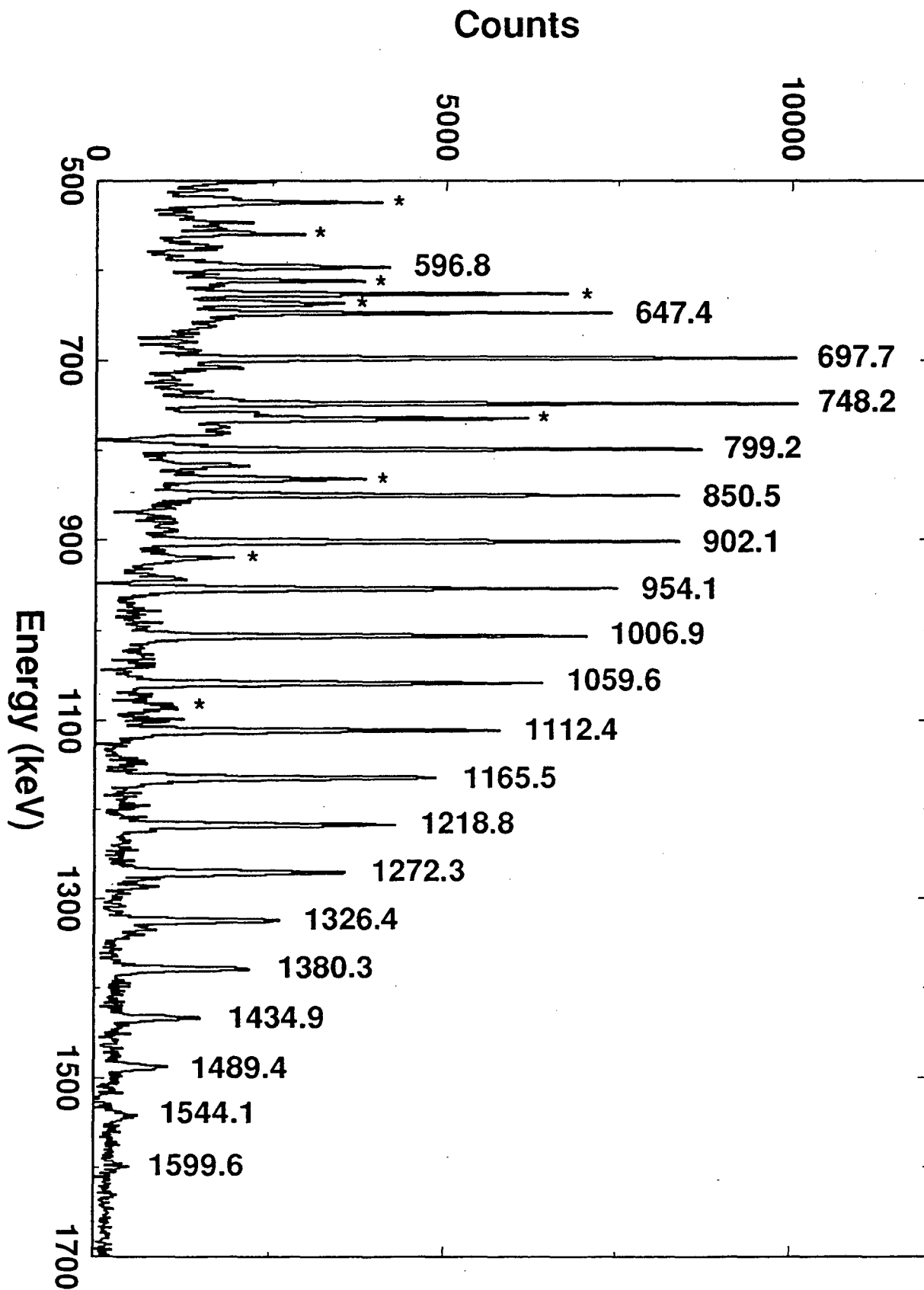
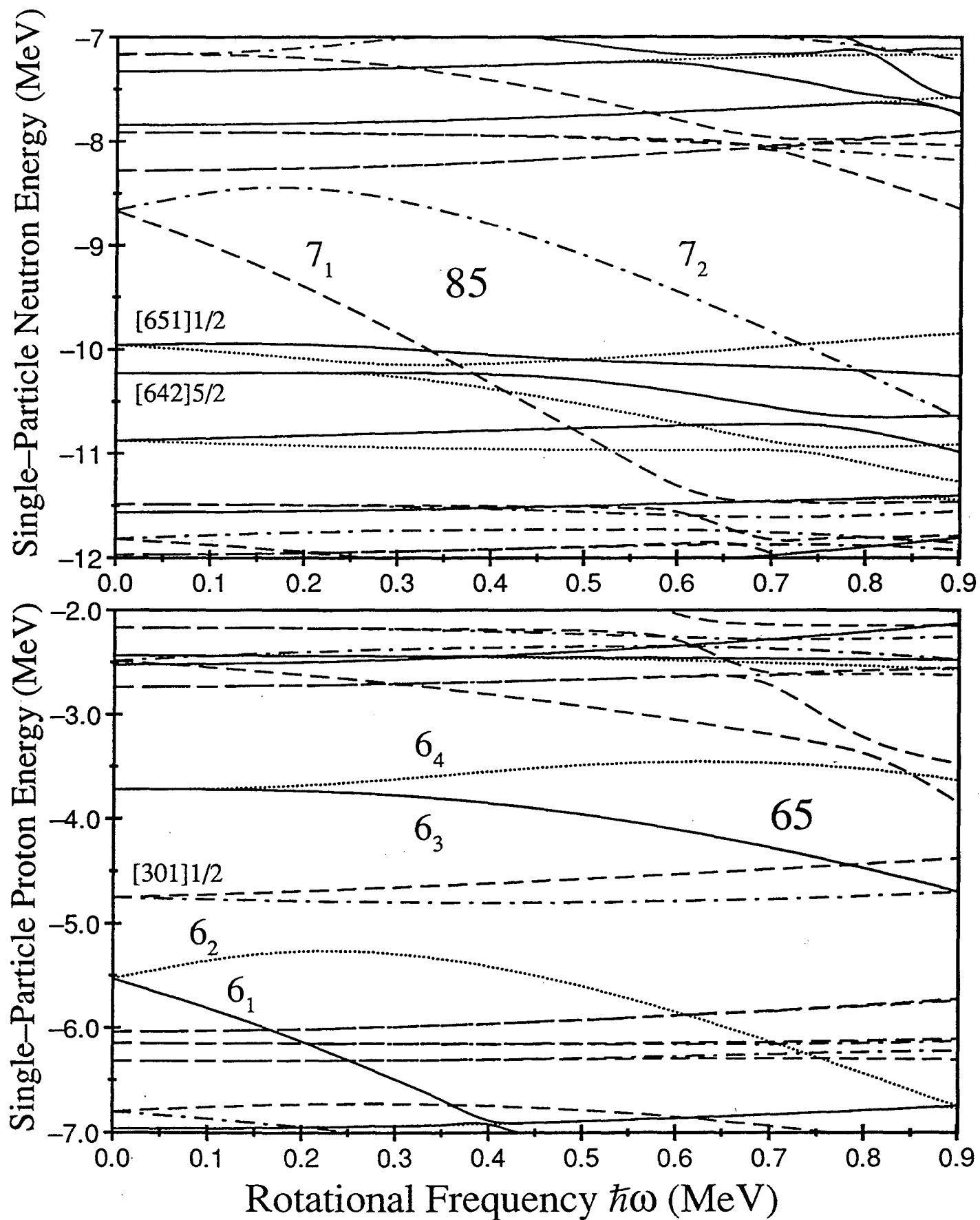


Figure 1

Figure 2



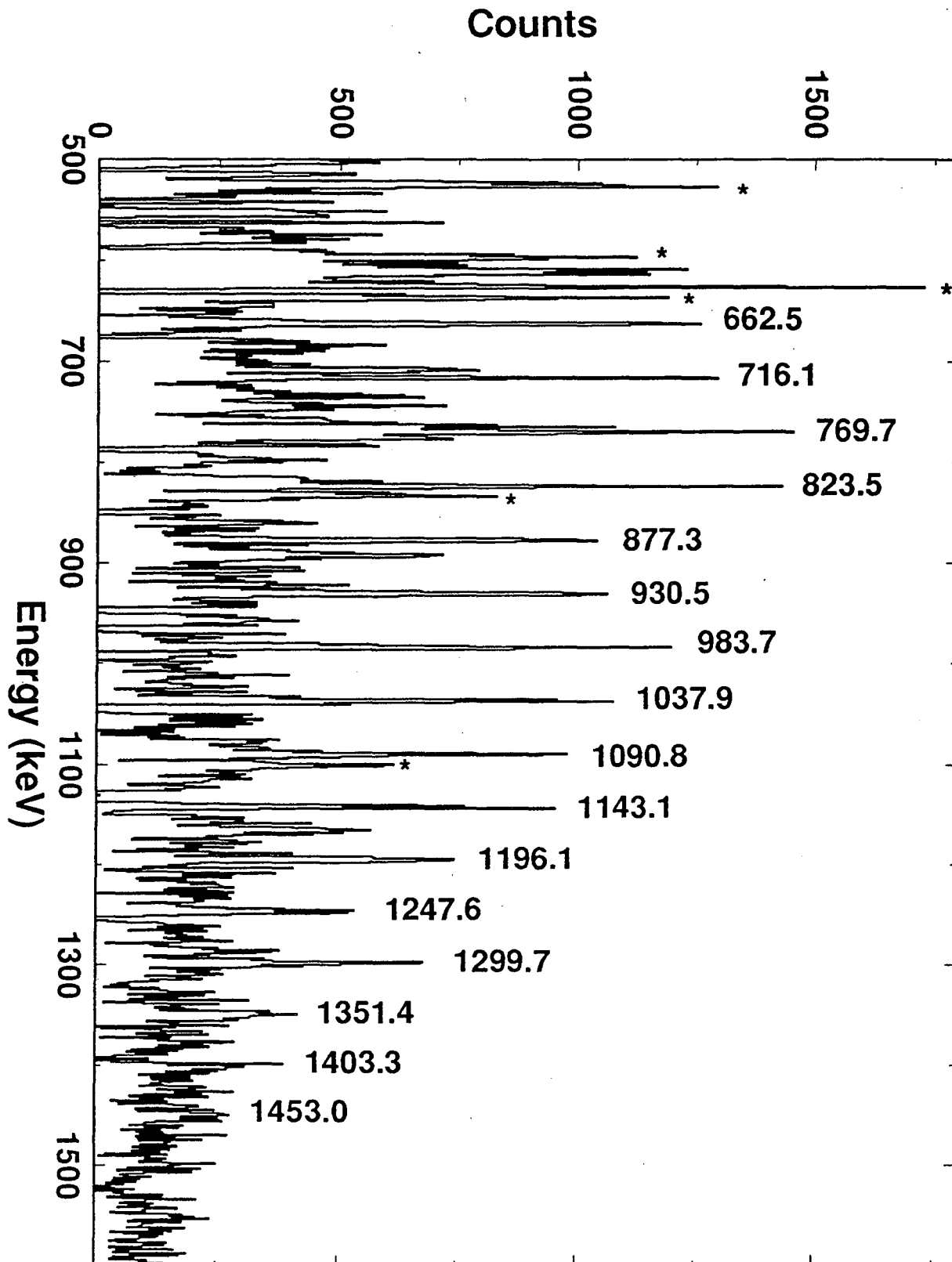
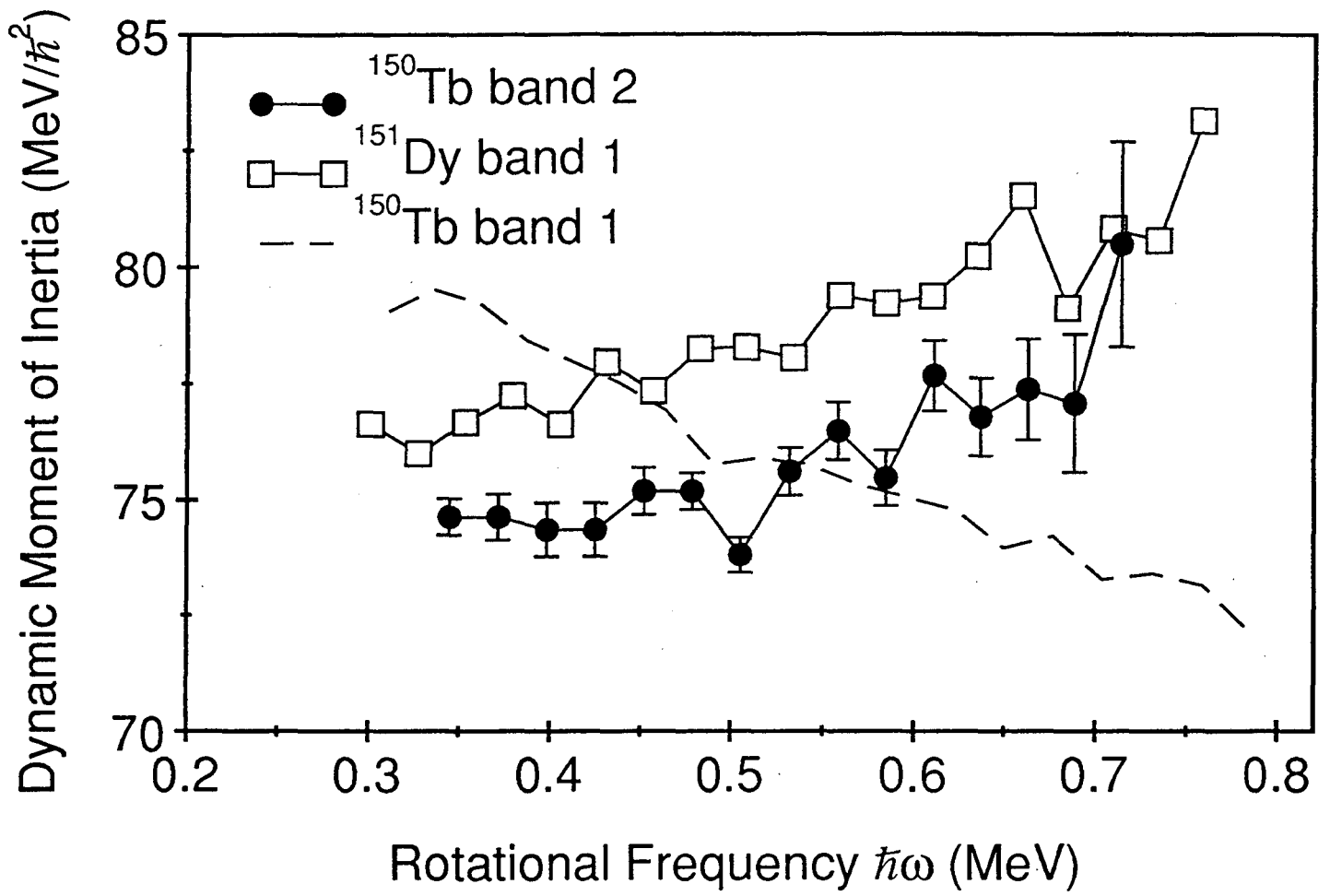


Figure 3

Figure 4



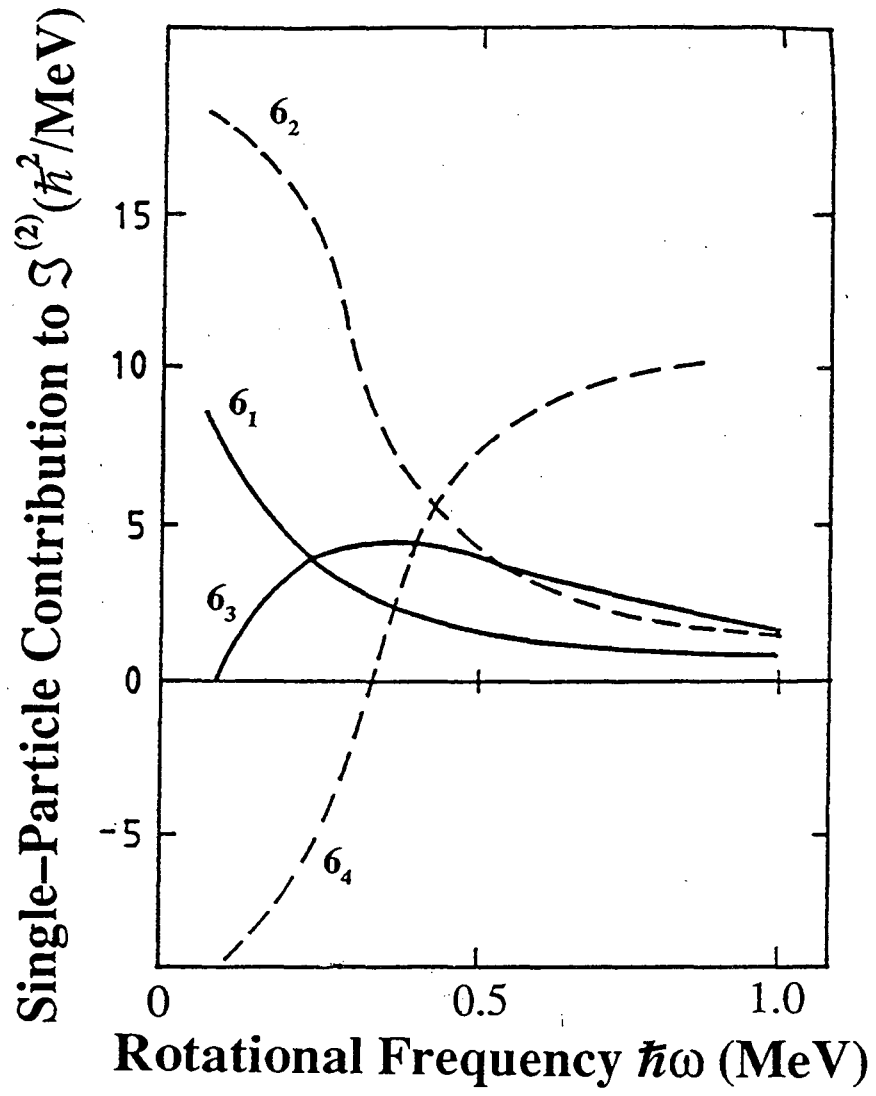


Figure 5
16

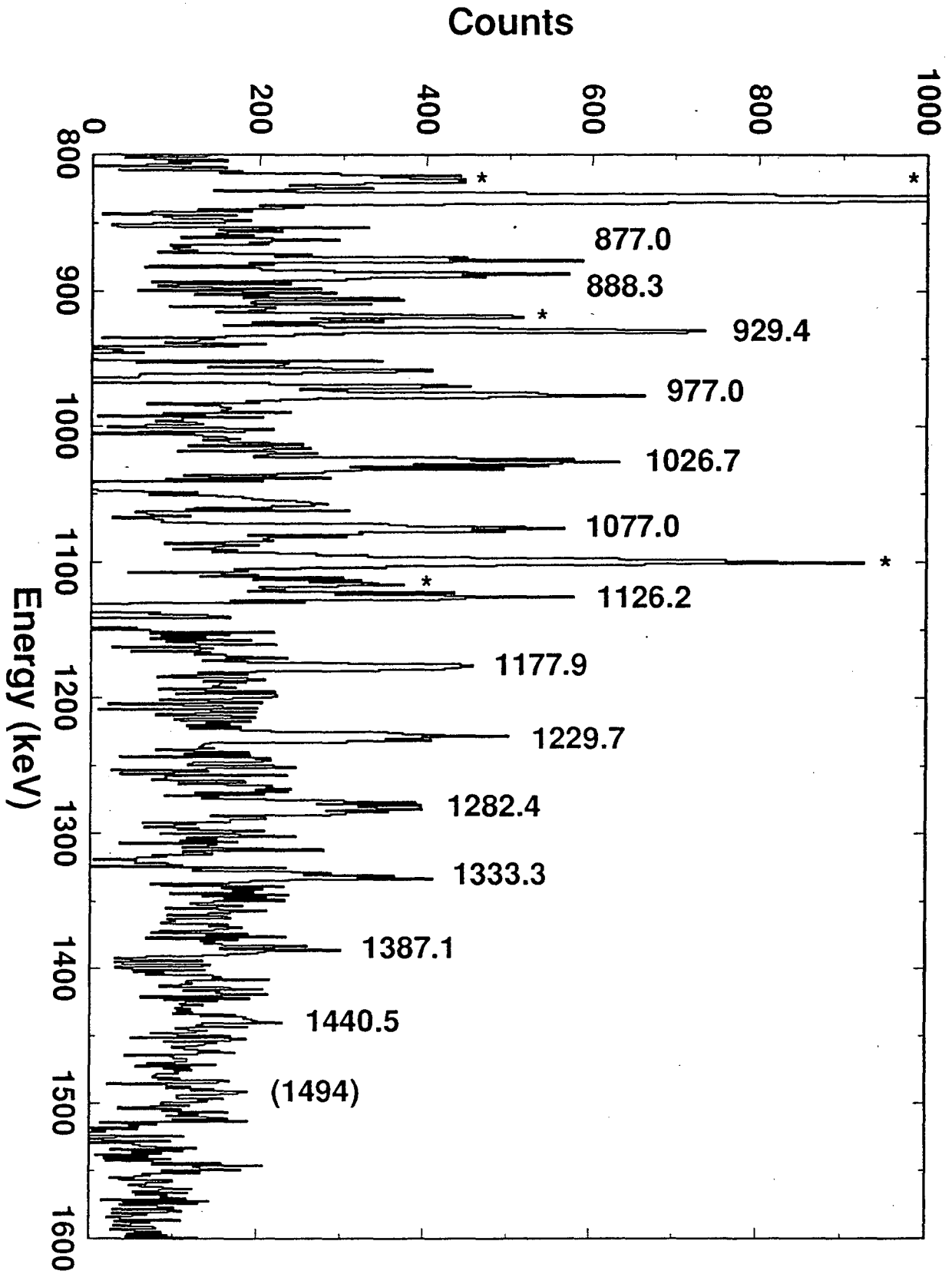
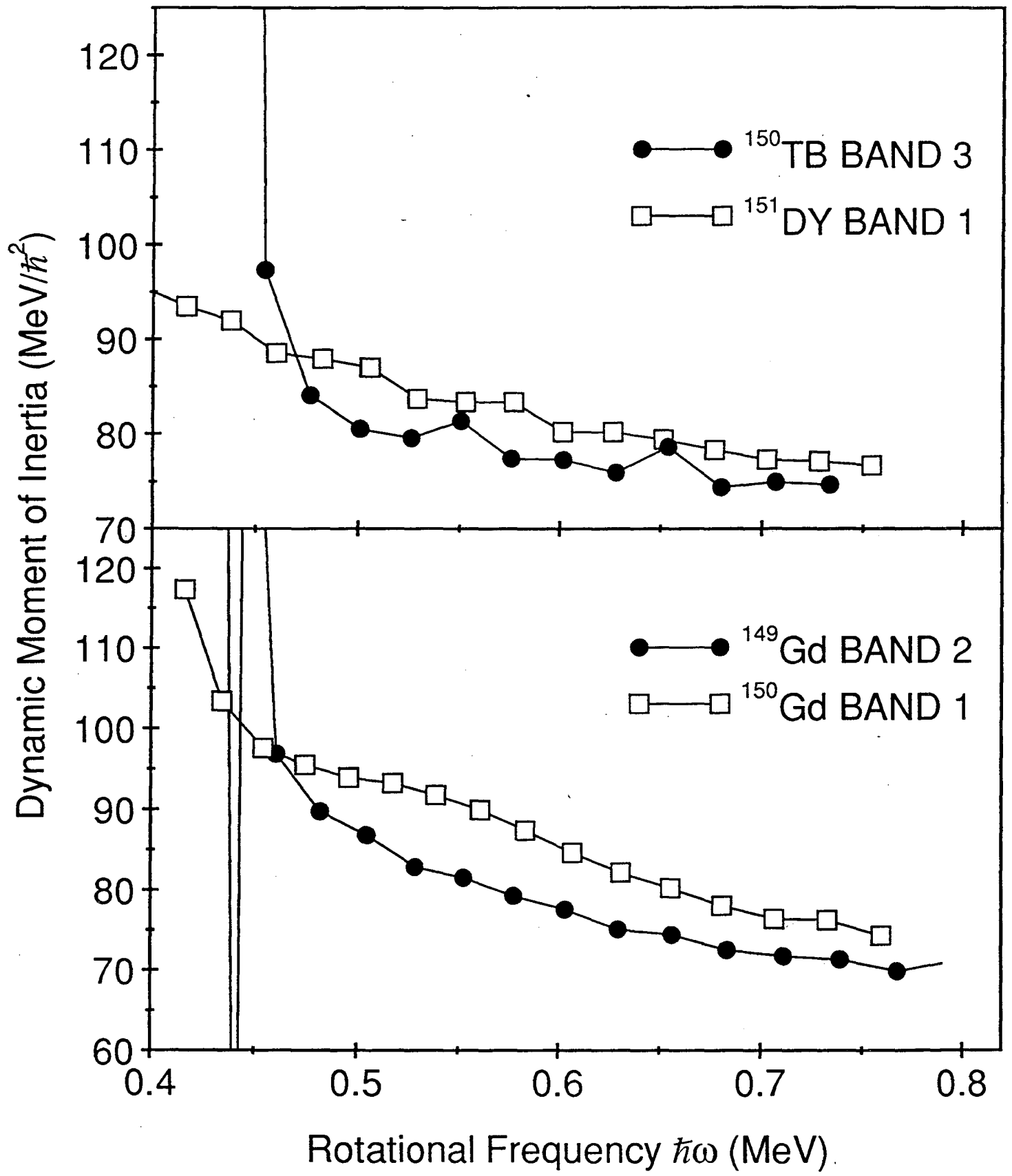


Figure 6

FIGURE 7



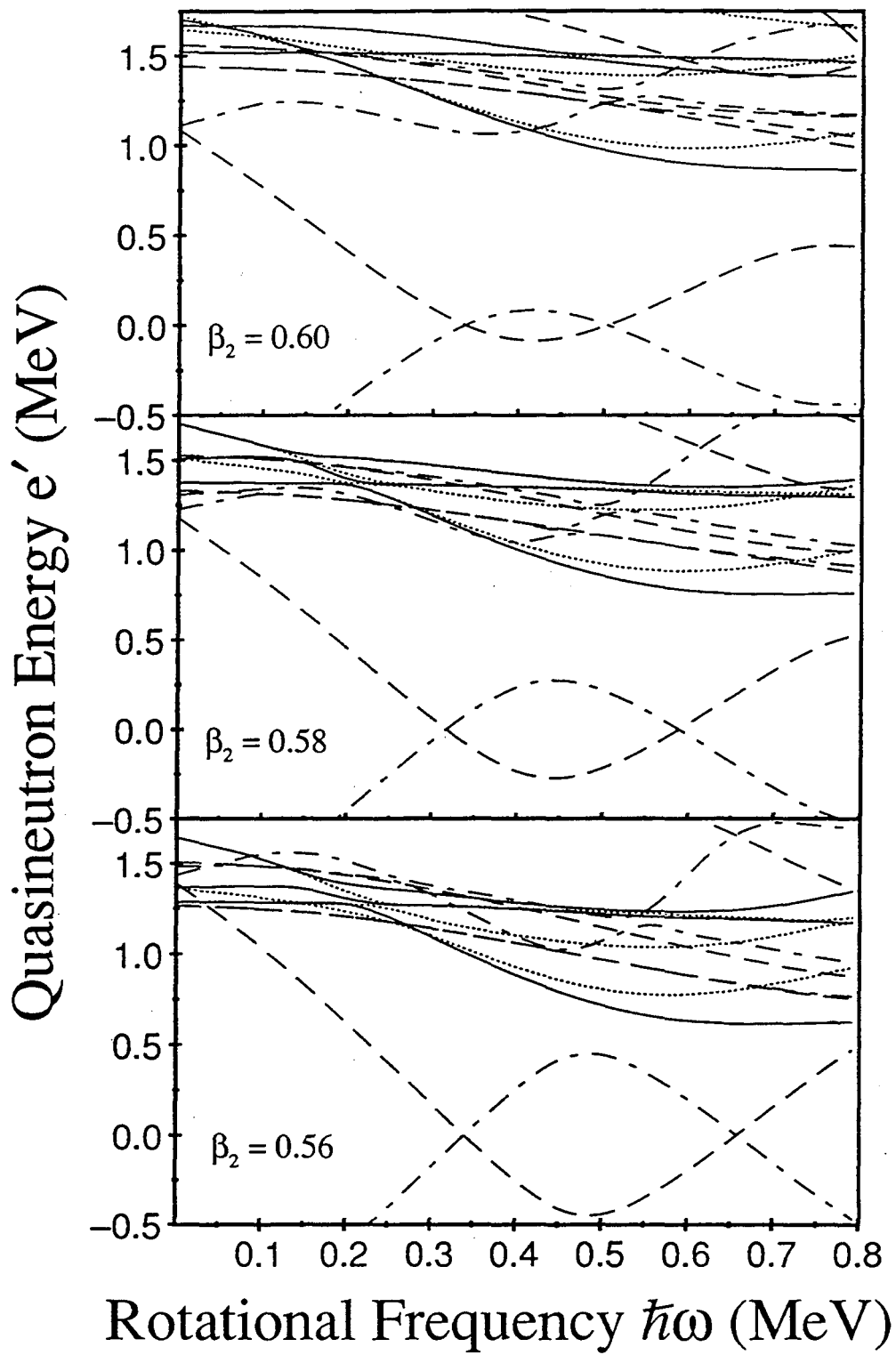


Figure 8

LAWRENCE BERKELEY LABORATORY
UNIVERSITY OF CALIFORNIA
TECHNICAL AND ELECTRONIC
INFORMATION DEPARTMENT
BERKELEY, CALIFORNIA 94720